

# **Analysis of the influence of climatic factors on the production of photovoltaic (PV) panels: case of the prefecture of Yomou, Republic of Guinea**

## **Abstract**

Despite its rich hydrological and rainfall potential, Yomou prefecture is one of the most energy-lagging cities in the forest region. This is why people choose to use solar panels as an energy source. Although the use of these panels is considered as a solution to the energy problems in Yomou, it is clear that climatic factors (such as: solar radiation, temperature, humidity and precipitation) have a negative impact on the performance of the installed panels. The aim of this work is to study the impact of climatic factors on the performance of photovoltaic energy production in order to identify the causes of solar energy production losses in this locality. Statistical analysis tools are used to assess annual and seasonal trends in climate variables. Use graphs to illustrate the variation and correlation between these factors and photovoltaic performance. The results show that the solar potential is high, especially during the dry season (January to April and November), providing optimal conditions for solar production. However, the rainy season (June to September) reduces the efficiency of photovoltaic panels due to increased diffuse radiation. To maximize energy production, technologies such as bifacial panels or solar tracking systems are recommended. It is also important to manage the tilt of the panels and take into account changes in light index (Kt) and seasonal temperature. The integration of storage solutions and the adaptation of the system to local conditions will ensure continuous energy production throughout the year. The relative humidity in the locality is on average 70%, peaking during the wet season (May to October) and decreasing during the dry season (November to April). These seasonal changes can affect the performance of photovoltaic panels, highlighting the importance of having systems adapted to local climatic conditions.

**Keywords:** Impact, performance, photovoltaic, energy, Yomou prefecture

## Introduction

Since the 1970s, the environment has been a major issue for everyone, due to the depletion of fossil fuel reserves, increasing energy demand and increasing environmental problems (**Hossein et al., 2020**). Thus, a growth in global electricity consumption has been observed in recent decades due to the development of industry, transport and means of communication (**Touil et Benoumhani, 2022**). However, renewable energies have taken a central place in meeting the demands of sustainable development since the beginning of the century (**Saoudi, 2018**). They remain essential for governments and scientists to participate in the energy mix policy of countries (**Singh et al., 2021**). Most of the electrical energy whose depletion time is estimated at a few decades is produced by combustion of non-renewable resources (coal, oil, gas, nuclear) (**Touil et Benoumhani, 2022**). The development of renewable and non-polluting energy sources is therefore topical (**Ounis, 2014**). Different renewable energy sources such as hydroelectric energy, wind energy, solar energy, biomass, geothermal energy and ocean energy can participate in the energy mix. In the global energy transition, solar energy is expected to play a vital role (**Allouhi et al., 2022**). Solar energy is seen as an essential solution to reduce energy dependence (**Lazaroiu et al., 2023**).

Photovoltaic solar energy comes from the direct transformation of part of solar radiation into electrical energy (**Zerdoudi et Chenni, 2015**). It is one of the most reliable and renewable energy sources used for electricity generation, which is based on the direct conversion of solar irradiation into electric current using semiconductors such as crystalline silicon (**Dida et al., 2020**). This energy conversion is carried out through a so-called photovoltaic (PV) cell based on a physical phenomenon called the photovoltaic effect which consists of producing an electromotive force when the surface of this cell is exposed to light (**Pankow, 2004**). The voltage generated may vary depending on the material used to manufacture the cell (**Zerdoudi et Chenni, 2015**). According to (**Toufik and Assia, 2014**), the photovoltaic (PV) effect is one of the ways of exploiting energy by transforming the energy of photons into electricity using solar cells.

Also, solar PV energy has experienced rapid growth globally in recent decades. China, the United States and India occupy a dominant position in this energy revolution (**Rahman et al., 2021**). According to the International Energy Agency (AIE) report, the global potential of solar PV reached 894 GW in 2022, making it the fastest growing PV technology (**International Energy Agency, 2023**). Solar energy takes center stage in global initiatives to reduce carbon emissions, with an average annual increase of 20% (**Publications, E. (Ed.). (2022)**).

Additionally, according to the 2022 Global Energy Survey, China continues to dominate the global solar energy market, with over 30% of new installations in 2021 (**International Energy Agency, 2023**).

The performance of a PV system strongly depends on climatic conditions, such as sunshine and temperature (**Toufik et Assia, 2014**). However, Africa could become a world leader in solar energy production by exploiting its immense irradiation and mining resource potential. According to (**Fouad et al., 2017**), the continent benefits from an average annual sunshine of 300 days, which makes it particularly conducive to the exploitation of this resource. However, Africa currently constitutes only a small proportion of the world's installed solar capacity, due to challenges such as lack of infrastructure, high upfront costs and sometimes inadequate regulations (**Thomas, 2014**). However, the African Development Bank (AfDB) 2020 believes that Africa has the potential to become a global leader in solar energy, but this requires considerable investment in infrastructure and coherent policies (**BAD, 2020**). According to the World Bank in 2021, with more than 600 million people without electricity in sub-Saharan Africa, solar could play a vital role in the sustainability of the continent's electrification (**FAO, 2018**).

Solar is a very powerful source of energy (**Touil et Benoumhani, 2022**). According to Observ'er 2004, the power of solar radiation at ground level is approximately 950 Watt/m<sup>2</sup>. Guinea Despite its high potential in terms of solar radiation (solar irradiation of 5.5 kWh/m<sup>2</sup>/day) and the adoption rate of this technology, is still very low. However, difficulties such as the lack of investments and effective public policies hamper its “Solar Guinea” expansion initiated in 2018 (**MEHG 2018**).

Forest Guinea, a region in which biodiversity is abundant, is located in southeastern Guinea. It faces many socio-economic challenges. Regarding energy, this area is very poorly electrified, with a large part of the population relying on traditional energy sources such as wood and charcoal, leading to deforestation and environmental degradation (**FAO, 2018**).

Solar energy can help fill this energy shortage, especially in isolated rural areas. However, the implementation of large-scale solar projects encounters various challenges such as: lack of infrastructure, the high cost of initial installations, as well as the absence of well-organized public policies (**FAO, 2018**).

In rural areas of Forest Guinea, dependence on traditional energy sources accentuates deforestation and contributes to local climate change. Like many rural regions of Guinea,

Yomou prefecture is deprived of electricity in all sub-prefectures. Current energy installations are not sufficient to meet the needs of the population, particularly in rural and peripheral areas (**Keita et al., 2024**). The introduction of solar panels can be a decentralized alternative, offering the possibility of producing electricity nearby without resorting to networks.

Thanks to the use of solar panels, local communities can acquire greater energy autonomy (**ADB, 2020**). This stimulates the economy by allowing access to electricity in schools, health centers and small businesses. In this way, solar energy can help improve the quality of life of populations and support the local economy (**BAD, 2020**).

Like many other rural areas of Guinea, the population of the Yomou prefecture has opted to turn to solar panels because of the many benefits they can obtain in terms of access to electricity (**FAO, 2018**). It should be noted that once solar panels are installed, local climatic conditions, such as irradiation, temperature, humidity and precipitation, have a detrimental effect on their efficiency over time.

Carrying out an in-depth study of climatic factors affecting the performance and yield of solar panels in Yomou prefecture is a necessity. For these reasons, the study of climatic factors would not only make it possible to better understand the technical challenges facing solar systems, but also to propose solutions adapted to the climatic reality of the region. This is how we chose to study the influence of climatic factors on the performance of PV photovoltaic panels in the Yomou prefecture. The general objective of this study is to identify the different effects of climatic parameters on the operation of PV installations in this prefecture.

## **2. Methodology**

### **2.1. Description of study area**

Yomou prefecture is located in the forest region of Guinea, in the southeast of the country. It is located between 7°45 north latitude and 9°16 west longitude. It borders Liberia to the south and east. It shares its boundaries with the prefectures of N'Zérékoré to the west and to the north, it is bordered by the prefecture of Macenta (Figure 1). Its climate is humid tropical. It has a dry season (November to April) and a rainy season (May to October) (**Djossou et al, 2024**), with an altitude varying between 40 and 48 meters above sea level, providing a slight climatic variation between low and high areas.

### **2.2. Data collection, processing and analysis**

The data used in this study were collected from the Meteonorm 8.2 site database for a period from January to December 2024 in Yomou prefecture.

The data were processed and analyzed using PVsyst 8.0.5 software. This allowed us to determine:

- **It is obtained by the following formula**

$$\delta = 23,44^\circ \times \sin\left(\frac{360}{365} \times (N + 10)\right) \quad (1)$$

Where: N is the day of the year (1 = January 1).

Solar height (h) is determined by equation (2)

$$h = \arcsin(\sin(\varphi) \sin(\delta) + \cos(\varphi) \cos(\delta) \cos(H)) \quad (2)$$

Where:  $\varphi$  is the latitude of the location and H is the solar hour angle.

**Solar azimuth (Az):**

$$Az = \arctan\left(\frac{-\cos(\delta)\sin(H)}{\sin(\varphi)\cos(\delta)\cos(H)}\right) \quad (3)$$

- **Calculation of global horizontal irradiation (GHI - Global Horizontal Irradiance)**

It is calculated by equation (4)

$$GHI = DNI \cdot (\cos\theta_z) + DHI \quad (4)$$

Where:

DNI: (Direct Normal Irradiance): Direct component, Solar energy arriving directly from the sun;

DHI: (Diffuse Horizontal Irradiance): Diffuse component; Solar energy that has been scattered by molecules, aerosols and clouds in the atmosphere;

$\theta_z$ : Zenith angle of the sun (angle between the sun and the vertical).

- **Determination of global, diffuse and global horizontal irradiation under clear sky**

For the determination of global, diffuse and global horizontal irradiation under clear sky, the Perez model (1990) was used. It uses data on the position of the sun, atmospheric transparency and optical thickness of the atmosphere. Takes into account parameters such as aerosols, water vapor and ozone.

The diffuse component can be determined by subtraction if the values of GHI and DNI (Direct Normal Irradiance) are available (see formula 5).

$$DHI = GHI - DNI \cdot \cos(\theta_z) \quad (5)$$

$\theta_z$ : Zenith angle of the sun.

- **Determination of Clarity Indices (Kt)**

The light index ( $K_t$ ) is a key parameter used to characterize solar radiation conditions at a given location. It is defined as the ratio of the horizontal global irradiation received at the ground ( $G_h$ ) to the extra-atmospheric irradiation ( $G_0$ ) at the top of the atmosphere (see formula below).

$$K_t = \frac{G_h}{G_0} \quad (6)$$

Calculation of extra-atmospheric irradiation ( $G_0$ )

$$G_0 = I_{sc} \cdot (1 + 0.033 \cdot \cos(\frac{2\pi n}{365})) \cdot \cos(\theta_z) \quad (7)$$

Where:

$I_{sc}$ : solar constant ( $1367 \text{ W/m}^2$ );

$n$ : day of the year (from 1 to 365);

$\theta_z$ : solar zenith angle calculated according to local time, latitude and longitude.

- **Determination of  $K_t$**

$$K_t = \frac{\int_{t_1}^{t_2} G_h dt}{\int_{t_1}^{t_2} G_0 dt} \quad (8)$$

Hourly values are often aggregated to obtain daily or monthly averages.  $K_t$  is a dimensionless number between 0 and 1.

- **Determination of the Incident Global Irradiation on a Fixed Inclined Plane**

The sum of the three components gives the overall incident irradiation on the inclined plane ( $I_t$ ) (see the formula below).

$$I_t = I_b + I_t + I_r \quad (9)$$

### **Determination of direct component ( $I_b$ )**

The direct incident irradiation on an inclined plane is calculated taking into account the angle of incidence ( $\theta$ ):

$$I_b = DNI \cdot \cos(\theta) \quad (10)$$

DNI: Direct normal irradiation.

$\cos(\theta)$ : Geometric factor between the solar vector and the normal vector to the inclined surface.

The angle of incidence  $\theta$  is given by:

$$\cos(\theta) = \sin(\delta) \cdot \sin(\phi) \cdot \cos(\beta) - \sin(\delta) \cdot \cos(\phi) \cdot \sin(\beta) \cdot \cos(\gamma) + \cos(\delta) \cdot \cos(\phi) \cdot \cos(\beta) \cdot \cos(h) + \cos(\delta) \cdot \sin(\phi) \cdot \sin(\beta) \cdot \cos(\gamma) + \cos(\delta) \cdot \sin(\beta) \cdot \sin(\gamma) \cdot \sin(h) \quad (11)$$

Where:

$\delta$  : Solar declination;

$\phi$  : Latitude of the site;

$\beta$  : Angle of inclination of the surface;

$\gamma$  : Azimuthal orientation of the surface (relative to the south).

To determine an inclined surface, the fraction of diffuse irradiation captured is given by:

$$I_d = DHI \cdot F_{sky} \quad (12)$$

DHI: Diffuse horizontal irradiation;

$$F_{sky} = \frac{1 + \cos(\beta)}{2} : \text{Sky view factor}$$

Some more advanced models (like the Perez model) subdivide the scattering into several components taking into account the anisotropy of the sky.

The reflected component is calculated from the global horizontal irradiation (GHI) and the albedo ( $\rho$ ):

$$I_r = GHI \cdot \rho \cdot F_{ground} \quad (13)$$

$$F_{ground} = \frac{1 + \cos(\beta)}{2} : \text{Ground view factor}$$

$\rho$  : Soil albedo (typically 0.2 for natural soil, 0.8 for snow).

The determination of the incident global irradiation on an inclined plane is essential to optimize photovoltaic or thermal systems.

Empirical methods like those of Perez, combined with simulation tools, allowed us to make reliable estimates adapted to local conditions.

- **Calculation of the average daily temperature ( $T_{moy}$ )**

The daily average temperature is obtained by the following formula.

$$T_{moy} = \frac{\sum_{i=1}^n T_i}{n} \quad (14)$$

$T_i$ : temperature measured at time  $i$ ,

n: total number of measurements taken during the day.

- **Calculation of average speed from data series**

The root mean square method is more accurate when wind direction varies because it takes into account the directional components of the wind. It is commonly used in meteorological studies (Equation 15).

$$\text{Root Mean Square Speed} = \sqrt{\frac{1}{n} \sum_{i=1}^n v_i^2} \quad (15)$$

- **Relative Humidity (RH):**

According to **Duffie et al., (1980)**, Relative Humidity is determined using the common formula:

$$HR = \frac{e}{e_s} \times 100 \quad (16)$$

Where:

HR: Relative humidity, expressed as a percentage (%);

e: Partial pressure of water vapor in air (Pa or hPa);

e<sub>s</sub>: Saturated vapor pressure at the same temperature (Pa or hPa).

### 3. RESULTS AND DISCUSSIONS

#### 3.1. Study of the trajectory of the sun in Yomou

Analysis of the solar trajectory in Yomou, combined with seasonal variations in sunshine, highlights significant opportunities to optimize solar energy production. The solar trajectory graph in this locality shows the movements of the sun according to legal time and seasons (**Figure 2**). June, with its longer sunshine duration (12 to 13 hours), is ideal for maximizing solar energy production, while in December, the reduced sunshine duration (around 11 hours) could lead to a drop in production. The azimuth and seasonal variations of the sun suggest that the tilt of photovoltaic panels must be adjusted according to the season to maximize their efficiency. The results obtained from the study of the sun's trajectory are consistent with those found by **Gaye et al. (2020)**, **Bonkaney et al. (2017)** and **Tan et al. (2018)** on the studies of

the influence of day length, cloudiness, and temperatures on the performance of photovoltaic panels. Also the results of **Bonkaney et al. (2017)** show a good correlation between the optimal inclination of the panels and the solar trajectories, which is essential to maximize the efficiency of solar installations in Yomou. Furthermore, the impact of cloud cover, as mentioned by **Tan et al. 2018**, highlights the need to model local climate conditions to better predict yield variations related to changing atmospheric conditions. Also adjusting the tilt of the panels, as well as taking into account cloudiness and temperature, can improve the efficiency of photovoltaic solar systems in Yomou.

### **3.2. Global, diffuse and global horizontal irradiances under clear sky in Yomou**

Analysis of irradiation data at Yomou highlights significant seasonal variations, directly influencing solar energy production. **Figure 3** shows global, diffuse and global clear-sky horizontal irradiances (synthetically generated from monthly averages). The annual sum of global horizontal irradiation (2075.2 kWh/m<sup>2</sup>) shows a strong solar potential, with maximum values between March and May, during the dry season, when direct solar radiation is abundant. On the other hand, a notable decrease is observed between June and September, due to the cloud cover associated with the rainy season. This period is characterized by a predominance of diffuse radiation, which represents approximately 48% of the annual global irradiation (996.5 kWh/m<sup>2</sup>). Then, global irradiation under clear skies (blue line) follows a regular trend, with peaks observed in March-May and a gradual decrease at the end of the year, representing the theoretical potential for energy production in the absence of clouds. This observation highlights that the dry season offers ideal conditions for photovoltaic systems, while the rainy season limits their performance due to the diffusion and absorption of solar rays. According to studies by **Gaye et al. (2020)** and **Tan et al. (2018)** on trends in tropical areas, the rainy season leads to an increase in diffuse radiation; which negatively affects the efficiency of photovoltaic panels.

### **3.3. Global normal horizontal irradiation of the beam under clear sky**

Figure 4 shows the overall normal horizontal irradiation of the beam under clear sky. Analysis of this figure shows a marked variation in solar irradiation in Yomou, depending on the seasons, with direct implications for photovoltaic energy production. The horizontal beam irradiation (black dots) reflects direct irradiation on a horizontal surface. Maximum values are observed during the dry season; which indicates ideal conditions for solar energy production with strong direct solar radiation. However, a significant decrease occurs during the rainy season, when clouds reduce the intensity of direct radiation. Also, the normal beam irradiation (inverted

triangles), representing the direct irradiation received on a surface perpendicular to the solar rays, follows a similar trend to that of the horizontal beam, but with overall higher values. This is explained by the more direct angle of incidence of the radiation on a perpendicular surface; which allows better capture of solar energy. However, as with horizontal irradiation, this component is reduced during the rainy season due to cloud cover.

Then, the global irradiation under clear skies (blue line), which gives an overview of the solar potential in the absence of clouds, confirms these trends, with maximum values during the dry season and a slight decrease during the rainy season. This illustrates the contrast between ideal conditions for solar energy production during the dry season and less favourable conditions during the rainy season. These results are consistent with those observed by **Diop et al. (2019)** in West Africa, where the rainy season reduces direct irradiation due to cloud cover. This reduction in direct radiation during the rainy season is a common phenomenon in tropical and subtropical areas, and it negatively affects the efficiency of conventional solar panels, which rely heavily on direct irradiation.

### **3.4. Incident global irradiation on the fixed inclined plane**

Figure 5 shows the global incident irradiation on the fixed inclined plane at Yomou. Analysis of this figure reveals significant variations depending on the seasons, directly impacting solar energy production. The annual incident irradiation on the fixed inclined plane is 2075.3 kWh/m<sup>2</sup>, with maximum values observed in February, March and April, corresponding to the dry season. This period benefits from ideal conditions for solar production, with high direct irradiation. In contrast, incident global irradiation under clear skies, representing the theoretical cloud-free potential, is constant throughout the year. Which highlights the optimal conditions in the absence of cloud cover.

Furthermore, the deviations between observed and theoretical values are particularly marked during the rainy season, with a significant decrease in irradiation due to the influence of clouds. This season is characterized by a predominance of diffuse radiation, which limits the production of solar energy, because traditional photovoltaic systems are more sensitive to direct irradiation than to diffuse irradiation. During the dry season, the irradiation on the inclined plane remains relatively stable, which favors increased solar energy production. These results are consistent with those obtained by **Omondi et al. (2020)** who worked on tropical regions, particularly in Asia and Latin America.

According to **Omondi et al. (2020)**, seasonality and weather conditions, especially cloud cover, play a determining role in solar energy production. These studies suggest solutions to optimize solar energy collection, such as the adoption of bifacial solar panels or solar tracking systems. These technologies make it possible to maximize the efficiency of photovoltaic systems by adjusting the orientation of the panels or by exploiting the light reflected by the ground.

### **3.5. Indice clarté (Kt)**

Figure 6 shows the daily evolution of the clarity index (Kt) of Yomou, with observations distributed throughout the year. Analysis of the clarity index (Kt) shows marked seasonal trends that directly influence the availability of solar radiation for photovoltaic energy production. The annual mean value of Kt is 0.6, indicating good transmission of solar radiation through the atmosphere. This suggests moderate availability of global solar radiation, with a significant share of direct radiation during dry periods. Indeed, during the dry season, the clarity index is generally more stable and higher (between 0.6 and 0.7), which means clear skies and optimal transmission of solar radiation. This season is therefore particularly favorable for the production of solar energy, with strong energy potential.

In contrast, during the rainy season, the clarity index decreases considerably, with values often below 0.5 and occasional drops to 0.2 or less. This is due to dense cloud cover and precipitation, leading to a predominance of diffuse radiation and a significant reduction in direct radiation. Very cloudy or stormy days, with occasional drops in Kt ( $<0.2$ ), reflect periods of heavy cloud cover or exceptional climatic events, such as thunderstorms or storms.

The extreme variations in the clearness index, with values exceeding 0.7 on very clear days, suggest that some days during the dry season may be almost cloud-free, allowing maximum direct solar radiation. This variability requires adequate planning and sizing of photovoltaic systems to maximize their efficiency. This result is close to that of **Diop et al. (2019)** who studied solar radiation conditions in West Africa, confirming similar clarity indices (0.55-0.65) and a strong influence of seasons, particularly monsoons and the Harmattan, on radiation conditions. Furthermore, **Omondi et al. (2020)** showed that semi-arid regions have more stable conditions for the clearness index, due to lower cloud cover.

### **3.6. Daily evolution of the average ambient temperature**

Analysis of the daily evolution of the average ambient temperature shows an annual average value of 25.6°C in Yomou, with notable seasonal variations (Figure 7). Higher temperatures are observed between February and April, reaching around 30°C, which corresponds to the dry

season period. On the other hand, from July to September, slightly lower temperatures are recorded, around 22-24 °C, due to increased humidity and cloud cover. This temperature trend is typical of tropical climates, influenced by monsoon and dry season cycles (**Diop et al. 2019**). This result is consistent with those of **Diop et al. (2019)** who found annual mean temperatures ranging between 24 and 30 °C in similar areas, with seasonal fluctuations due to the effects of monsoon winds and the Harmattan. Also, **Omondi et al. (2020)** note that in equatorial regions with high humidity, temperatures can cause a significant drop in the performance of photovoltaic panels.

### **3.7 Daily observation of average wind speed**

Figure 8 shows the daily evolution of the average wind speed over a year, with the different observations. Analysis of the figure indicates that the average annual wind speed is 2 m/s, which corresponds to a low intensity wind, typical of tropical areas. The speed peaks, reaching up to 6-7 m/s, occur mainly in February, June and July, coinciding with atmospheric disturbances in the wet season, particularly linked to monsoon systems.

Wind speeds vary significantly throughout the year, with periods of calm, particularly between October and December, when speeds are often less than 2 m/s. This indicates a predominance of calmer conditions, favourable to a more stable atmosphere. This irregular distribution of speed peaks suggests a strong influence of local climate regimes. The Harmattan at the beginning of the year and the monsoon in the wet season play a major role in these fluctuations. The results observed in Yomou are consistent with those of **Diop et al. (2019)**, who observed similar wind regimes in forested areas of West Africa. Seasonal variations in wind speed in Yomou, with peaks at the beginning and end of the year, are also found in the work of **Diop et al. (2019) and Omondi et al. (2020)**, who link these fluctuations to the effects of the Harmattan and the monsoon. Although average wind speeds are relatively low, periods of strong wind can have implications for the stability and durability of solar infrastructure. A thorough analysis of wind peaks would allow for better design of mounting structures for photovoltaic panels to protect them from high winds, while maximizing their output during calm periods.

### **3.8. Relative humidity**

Figure 9 shows a daily variation in relative humidity over a full year, with an annual average of 70%. It illustrates an annual variation in relative humidity, with an average of 70%. Humidity is low (40-60%) during the dry season, gradually increases to a maximum (80-90%) during the rainy season, then decreases at the end of the year. This trend reflects tropical climate cycles,

influenced by the Harmattan and monsoons. These results are consistent with those of **Diop et al. (2019)**, who observed similar variations in West Africa. However, high humidity during the rainy season can reduce the efficiency of PV panels by decreasing direct solar irradiation, as confirmed by **Omondi et al. (2020)**. It is therefore recommended to adapt solar systems to these variations, in particular by integrating humidity-resistant technologies and planning regular maintenance during humid periods.

#### **4. Conclusion**

In this study, we analyzed the influence of climatic factors on the performance of photovoltaic panels. The results obtained are as follows:

- Analysis of Yomou's climatic conditions shows that there is enormous potential for solar energy production, especially during the dry season.
- The use of solar energy is optimal in January, April and November, but during the rainy season the efficiency of photovoltaic panels decreases due to increased diffuse radiation.
- Managing panel tilt and integrating advanced technologies such as bifacial panels or solar tracking systems are promising solutions to maximize energy efficiency.
- The clarity index (Kt) reveals significant seasonal fluctuations, with phases of reduced clarity during the rainy season, which requires consideration of local conditions when designing photovoltaic systems.
- The importance of thermal management and structural design is accentuated by the temperature fluctuations and reduced wind speed in Yomou, in order to improve the efficiency of solar systems while ensuring their robustness in the face of severe weather conditions. To optimize solar energy production, it is essential to incorporate storage devices, consider seasonal fluctuations when planning installations, and design systems that match local conditions. This ensures stable and optimal production throughout the year.

## References

- African Development Bank (2020).** *Harnessing Solar Energy for Economic Growth in Africa*. Abidjan: AfDB Publications. Disponible en ligne : <https://www.afdb.org/>
- Allouhi A., Rehman S, Buker M.S., Zafar S. (2022) Up-to-date literature review on Solar PV systems: Technology progress, market status and R&D, *Journal of Cleaner Production*, 362, ISSN 0959-6526, <https://doi.org/10.1016/j.jclepro.2022.132339>
- Banque Africaine de Développement (BAD, 2020). *Powering Africa's Energy Future: Harnessing Renewable Energy Potential*.
- Bonkaney, A.L., Madougou, S. and Adamou, R. (2017) Impact of Climatic Parameters on the Performance of Solar Photovoltaic (PV) Module in Niamey. *Smart Grid and Renewable Energy*, 8, 379-393. <https://doi.org/10.4236/sgre.2017.812025>
- Dida M., Boughali S., Bechki D., Bouguettaia H. (2020) Output power loss of crystalline silicon photovoltaic modules due to dust accumulation in Saharan environment. *Renewable and Sustainable Energy Reviews* 124 (2020) 109787. <https://doi.org/10.1016/j.rser.2020.109787>
- Diop, S., Ndiaye, A., & Faye, A. (2019) The role of solar energy in Africa's energy transition. *Energy Reports*, 5, 1123-1135.
- Djossou, J., Mathos K. P., Zinsou H. L., Yombouno F. M., and Camara N. (2024) "Impact of the ITF Relationship and the Onset of Rainfall on Precipitation in the Republic of Guinea". *International Journal of Environment and Climate Change* 14 (12):1-12. <https://doi.org/10.9734/ijec/2024/v14i124602>
- Duffie J. A. and Beckman W. A. (1980) "Solar Engineering of Thermal Processes," NASA STI/Recon Technical Report A, 81, 928.
- Organisation des Nations Unies pour l'alimentation et l'agriculture (FAO, 2018).** *The State of the World's Forests 2018: Forest Pathways to Sustainable Development*.
- Fouad M.M., Shihata L. A., Morgan ElSayed I. (2017) An integrated review of factors influencing the performance of photovoltaic panels, *Renewable and Sustainable Energy Reviews*, 80, 1499-1511. <https://doi.org/10.1016/j.rser.2017.05.141>
- Gaye, C., Ndiaye, A., Diop, S., & Faye, A. (2020). Impact of temperature on solar PV efficiency in tropical regions. *Journal of Energy Research*, 45(2), 112-125.
- Hussein A., Kazema B., Miqdam T. Chaichanc , Ali H.A. Al-Waelib , K. Sopianb. A novel model and experimental validation of dust impact on grid-connected photovoltaic system performance in Northern Oman. *Solar Energy* 206 (2020) 564–578.  
<https://doi.org/10.1016/j.solener.2020.06.043>
- International Energy Agency (2023).** *World Energy Outlook 2023*. Paris: IEA Publications. Disponible en ligne : <https://www.iea.org/reports/world-energy-outlook-2023>

Keita O., Diallo A. M., Camara Y., Rafi M. and Ouedraogo D. (2024) “Influence of Meteorological Parameters on the Performance of Solar Panels in the Urban Commune of Nzérékoré, Guinea”, *Asian Journal of Science and Technology*, 15, (02), 12876-12881.

Lazaroiu G. C., Roscia M. (2023) Key Elements to Create Renewable Energy Communities (REC). International Conference on Renewable Energy Research and Applications (ICRERA). <https://doi.org/10.1109/ICRERA59003.2023.10269406>

**Ministère de l'Énergie et de l'Hydraulique de Guinée (2018).** *Plan stratégique pour le développement des énergies renouvelables en Guinée.*

Ndiaye A. (2013). Étude de la dégradation et de la fiabilité des modules photovoltaïques - Impact de la poussière sur les caractéristiques électriques de performance. Thèse de Doctorat. Université Cheikh Anta Diop de Dakar. *Energies Renouvelables et Systèmes Electriques*. 19 pages.

Omondi B. A., Soko M. M., Nduwimana I., Delano R. T., Niyongere C., Simbare A., Kachigamba D., Staver C. (2020) The effectiveness of consistent roguing in managing banana bunchy top disease in smallholder production in Africa. *ant Pathology*, 69, 1754-1766. <https://doi.org/10.1111/ppa.13253>

Ounis Tarek Diab (2014) Protection des panneaux solaires. Mémoire de master physique, Option : Sciences des Matériaux. UNIVERSITE L'ARBI BEN MHIDI (OUM EL BOUAGHI).

Pankow Y. (2004) « Etude de l'intégration de la production décentralisée dans un réseau basse tension, application au générateur photovoltaïque », Thèse de Doctorat, Ecole Nationale Supérieure d'Arts et Métiers, ENSAM Lille, France.

Publications, E. (Ed.). (2022). *The Europa Directory of International Organizations 2022* (24th ed.). Routledge. <https://doi.org/10.4324/9781003292548>

Rahman A., Aziz T., Masood- N.-Al., Deeba S. R., (2021) A time of use tariff scheme for demand side management of residential energy consumers in Bangladesh. *Energy Reports*, 7, 3189-3198. <https://doi.org/10.1016/j.egy.2021.05.042>

Saoudi K. (2018) Stabilisateurs intelligents des systèmes électro-énergétiques. Université FERHAT ABBAS — SETIF1 UFAS (ALGERIE)

Singh, J., Rahman, S.A., Ehtesham, N.Z. *et al.* SARS-CoV-2 variants of concern are emerging in India. *Nat Med* 27, 1131–1133 (2021). <https://doi.org/10.1038/s41591-021-01397-4>

Tan, Q., Huang, B., Niu, D., & Zhang, X. (2018). Effects of environmental factors on the efficiency of photovoltaic modules: A review. *Renewable Energy*, 120, 377-389.

Thomas M (2014). Caractérisation de panneaux solaires photovoltaïques en conditions réelles d'implantation et en fonction des différentes technologies. Thèse de Doctorat. Université Paris-sud. 24 pages.

Toufik S., Assia A. (2014) 'Etude de l'impact des facteurs climatiques (Température, ensoleillement) sur la puissance des cellules photovoltaïques', SN02, Ecole Normale Supérieure d'Enseignement technologique de Skikda, Skikda, Algérie.

Touil H. et Benoumhani A. (2022). Contribution à la protection des panneaux solaires contre le vent de sable.

<file:///C:/Users/DOCTEUR/Desktop/Diallo/M%C3%A9moire%20Master%202022>

Zerdoudi A., Chenni R. (2015). Etude de l'influence des différents paramètres sur un module photovoltaïque. Sciences & Technologie A – N°41, 49-54.

# FIGURES

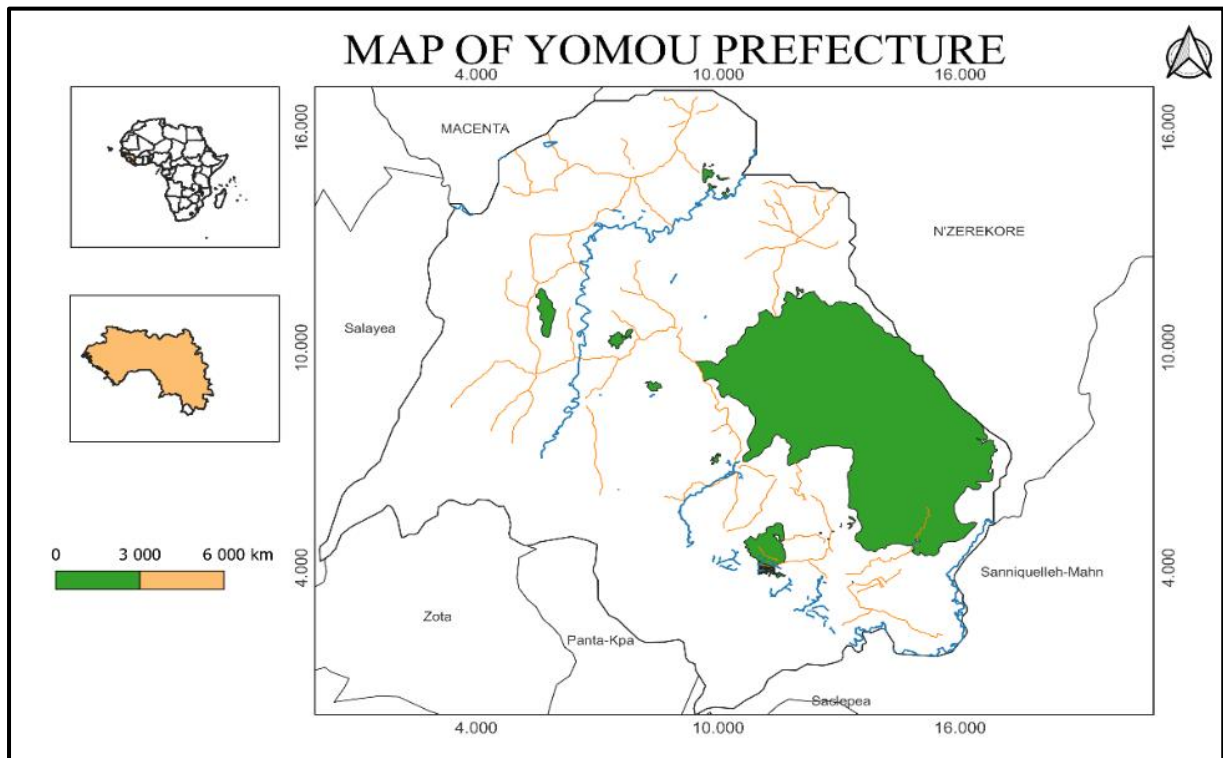


**Figure 1:** Map of Yomou prefecture

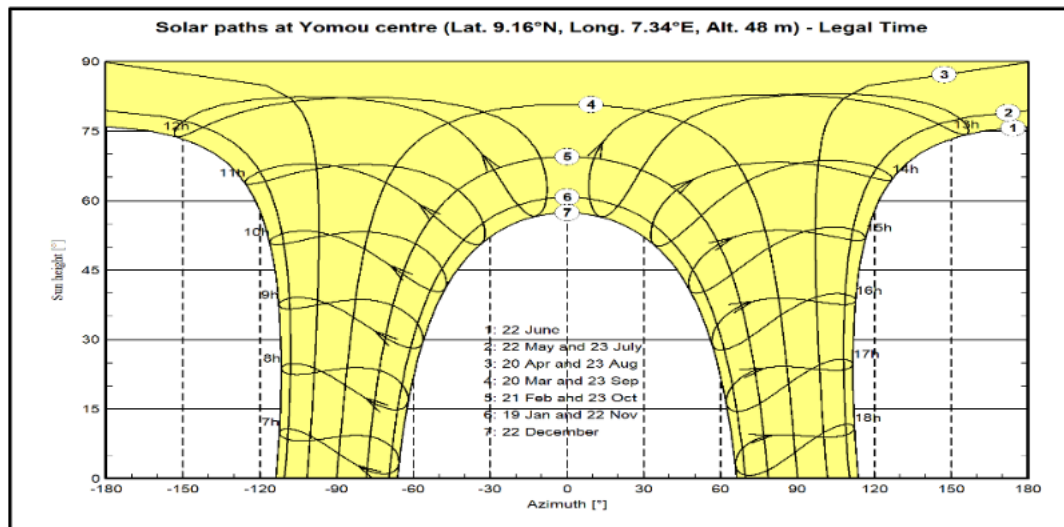


**Figure 2:** Sun trajectory in Yomou prefecture

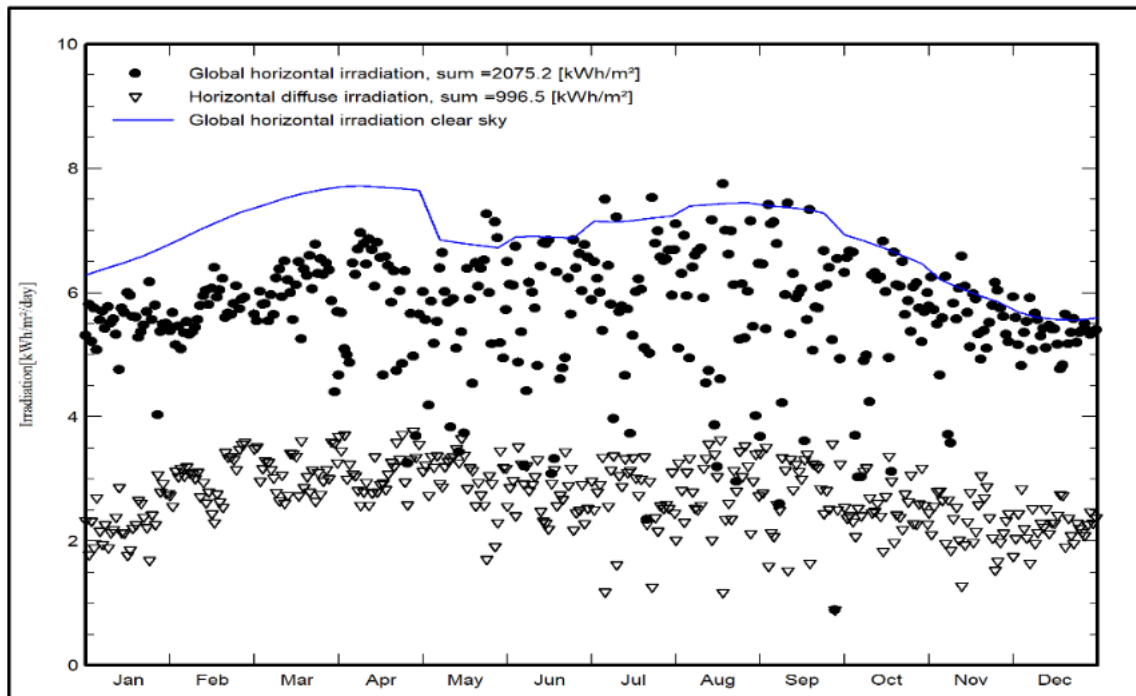


Figure 3: Global, diffuse and global horizontal irradiancies under clear sky

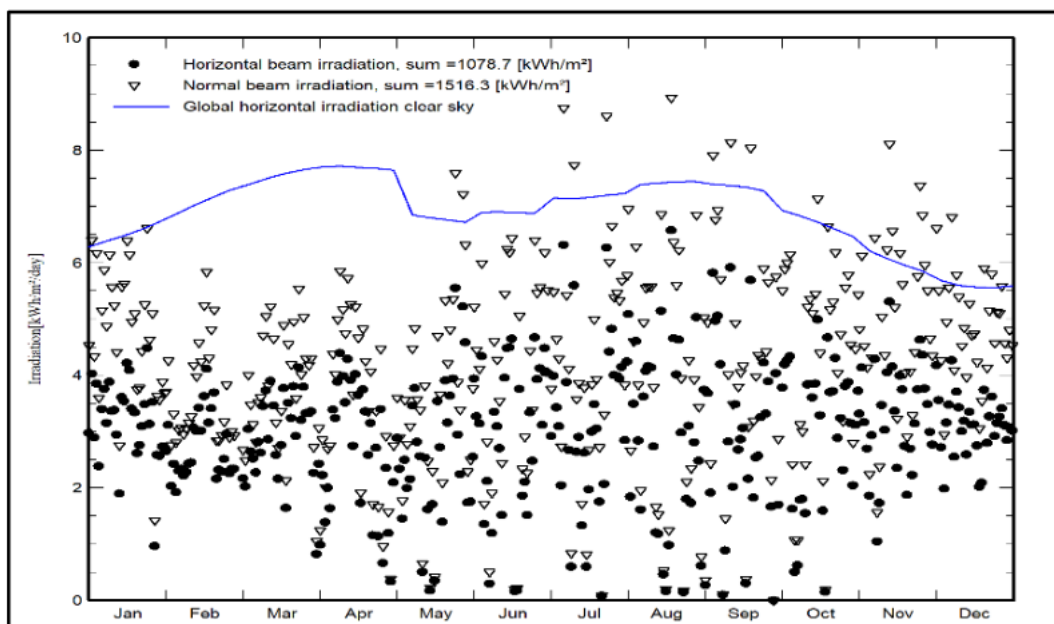
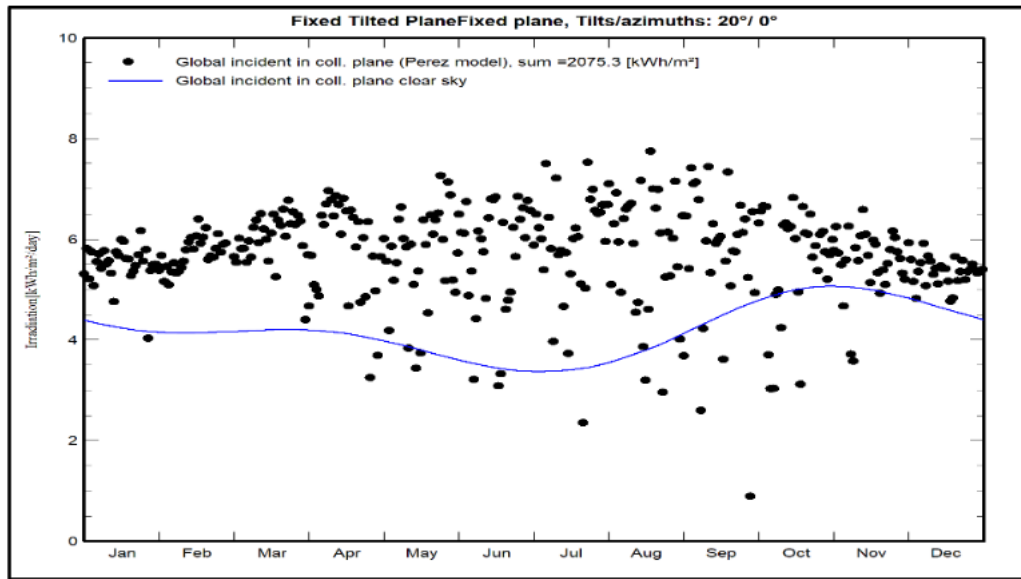
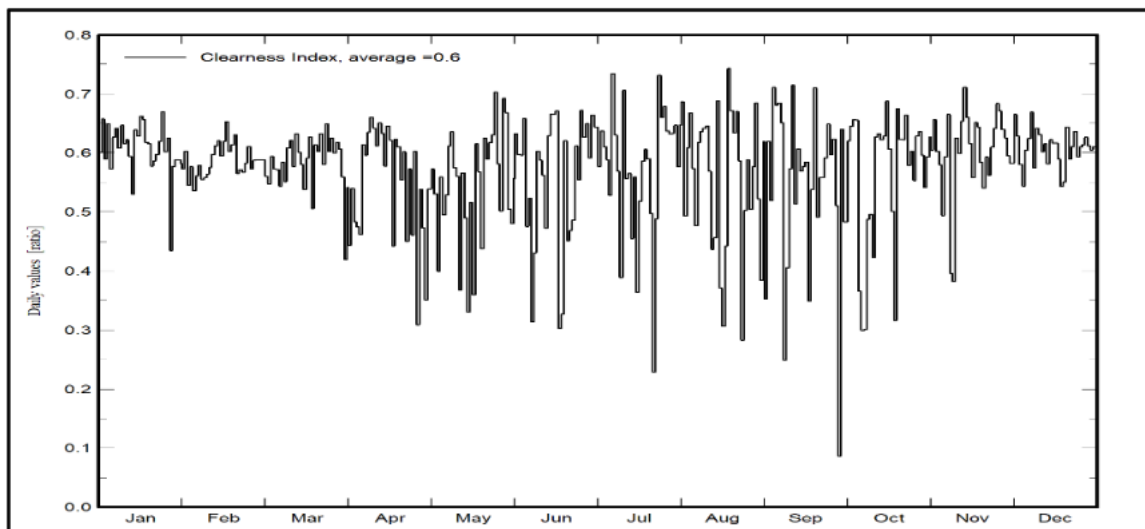


Figure 4: Global normal horizontal irradiation of the beam under clear sky



**Figure 5:** Incident global irradiation on the fixed inclined plane



**Figure 6:** Daily evolution of the clarity index (Kt)

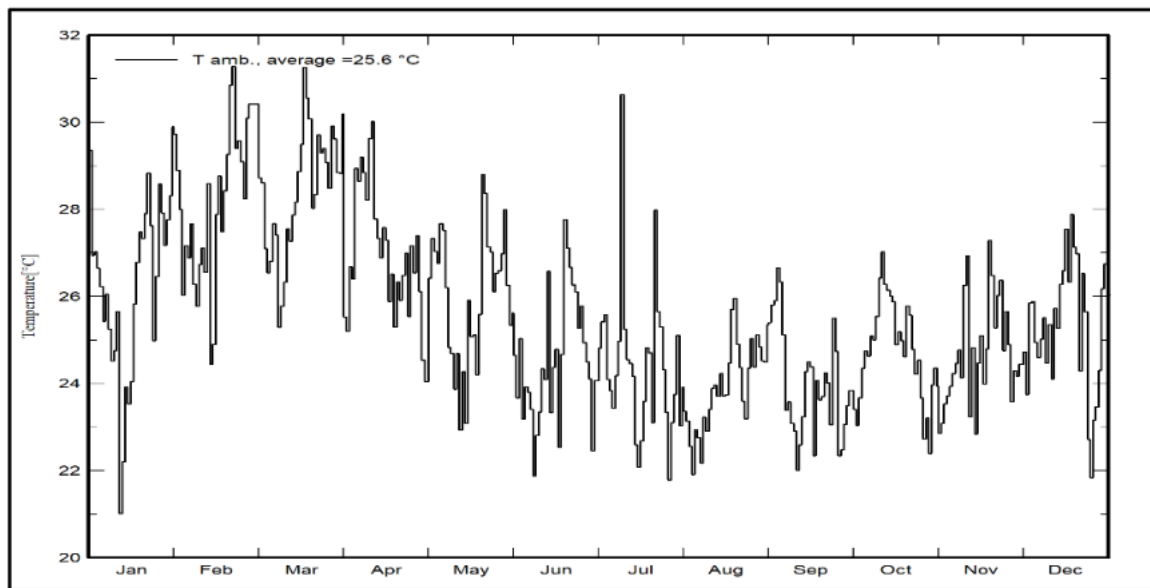


**Figure 7:** Daily evolution of the average ambient temperature

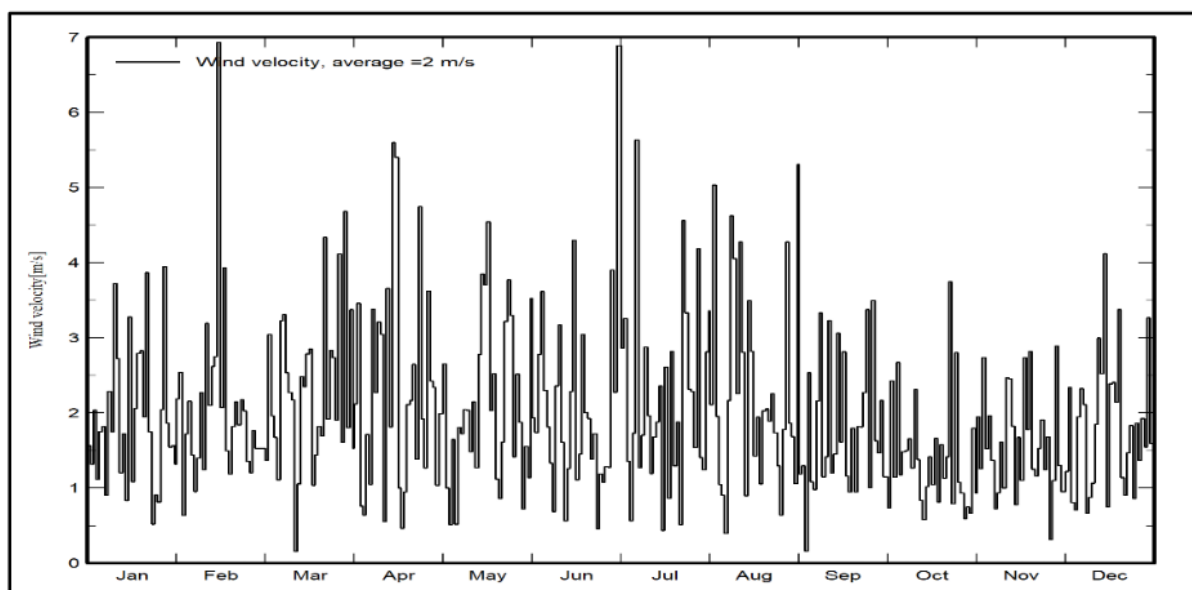


**Figure 8:** Daily observation of average wind speed

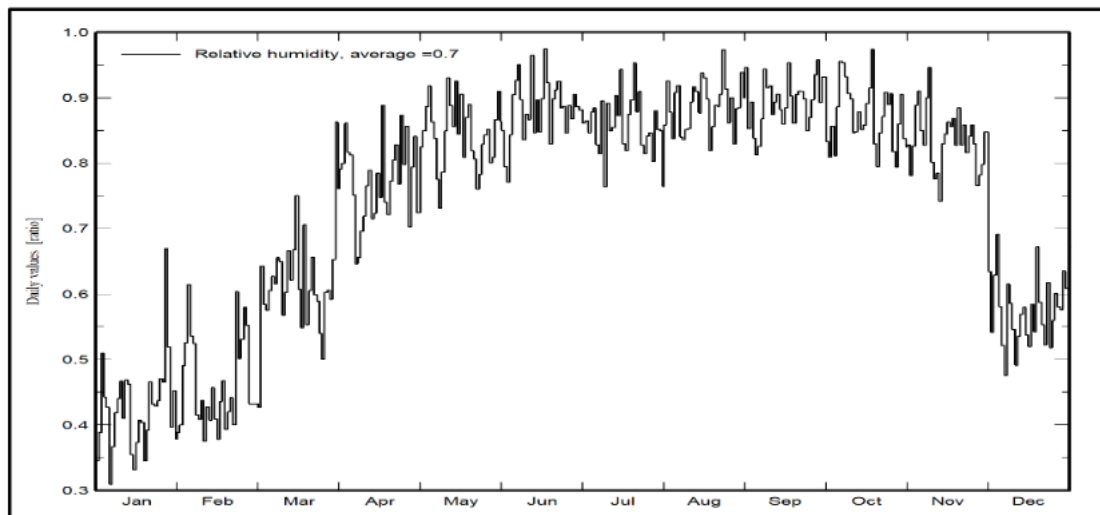


**Figure 9:** Daily average relative humidity